Towards closing the window of primordial black holes as dark matter: The case of large clustering

Torsten Bringmann[*]

Department of Physics, University of Oslo, Box 1048, N-0371 Oslo, Norway

Paul Frederik Depta,[†] Valerie Domcke,[‡] and Kai Schmidt-Hoberg[§]

Deutsches Elektronen-Synchrotron DESY, Notkestraße 85, D-22607 Hamburg, Germany

The idea of dark matter in the form of primordial black holes has seen a recent revival triggered by the LIGO detection of gravitational waves from binary black hole mergers. In this context, it has been argued that a large initial clustering of primordial black holes can help alleviate the strong constraints on this scenario. In this work, we show that, on the contrary, with large initial clustering the problem is exacerbated and constraints on primordial black hole dark matter become overwhelmingly strong.

I. INTRODUCTION

Soon after realizing that black holes (BHs) could form in the early radiation-dominated Universe [1–3] from the gravitational collapse of large density fluctuations, it was pointed out that such objects may even contribute appreciably to the total matter density [4]. An obvious question is therefore whether these primordial black holes (PBHs) could explain *all* of the cosmologically observed dark matter (DM); see Refs. [5,6] for recent reviews. This idea has seen greatly renewed interest [7–11] after the discovery of binary mergers by the Advanced Laser Interferometer Gravitational-Wave Observatory (LIGO) [12–15], proving the existence of $\mathcal{O}(10\,M_\odot)$ BHs with so far an unclear origin.

Constraints on the allowed DM fraction f_{PBH} of PBHs derive from a large number of observations and have been explored for a vast range of mass scales; see Refs. [5,6,10] for an overview. While there seems to be a broad consensus that $f_{\mathrm{PBH}} \sim 1$ is essentially excluded for black hole masses $m_{\mathrm{PBH}} \gtrsim 10^{-10}\,M_\odot$ when assuming a homogeneously distributed population of PBHs with a single mass, this general picture changes when either of these conditions is not met. Intriguingly, this also opens the window of PBH masses consistent with the LIGO observations by circumventing the stringent constraints from microlensing and from the cosmic microwave background (CMB) [16] (see, however, [17,18]).

Clustered PBH distributions have been argued to arise generically in Refs. [19,20], possibly explaining the

existence of supermassive BHs [21,22]. Only recently it was realized that significant clustering is in fact *not* expected for Gaussian primordial fluctuations [23,24], as predicted by vanilla models of cosmic inflation. However, highly clustered PBH distributions could still plausibly arise, e.g., in the presence of sizable primordial non-Gaussianities [25] or from the collapse of domain walls [26]. In this work we choose to be agnostic about the possible origin of large PBH clustering. Instead, we demonstrate that in such a situation $f_{\mathrm{PBH}} \sim 1$ is in fact still excluded over a wide mass range, thereby closing this possibly last loophole for all DM consisting of PBHs with masses larger than $10^{-10}\,M_\odot$.

The initial clustering of PBHs is indeed a key parameter to understanding the phenomenology of PBH DM, affecting merger rates [27,28], the subsequent structure formation [29], and the interpretation of observational bounds [16]. Here we take a pragmatic and phenomenological approach by parametrizing the clustering as a constant, free parameter on the scales of interest. We point out that, for the large PBH clustering discussed in the literature, the expected merger rates easily exceed one per binary and Hubble time. We demonstrate that multiple subsequent mergers severely constrain PBH DM as a possible explanation of the LIGO events because of (i) the expected (as compared to observed) merger rate, (ii) the impact of the additional radiation component in gravitational waves (GWs) on both CMB and large-scale structure observations, and (iii) a present-day stochastic GW background (SGWB) exceeding the sensitivities of current ground-based (or future space-based) observatories.

This article is organized as follows. We start by describing the GW spectrum and energy density from cosmological PBH mergers, before discussing how the merger rate

[*]torsten.bringmann@fys.uio.no
[†]frederik.depta@desy.de
[‡]valerie.domcke@desy.de
[§]kai.schmidt-hoberg@desy.de

critically depends on the initial PBH clustering. We then introduce a cascading merger scenario to capture the effects of large clustering and, hence, high merger rates. We derive the resulting contributions to the stochastic GW background and the relativistic energy density in GWs, using the cosmological parameters from Ref. [30] whenever relevant. Along with the actual event rate observed by LIGO, we use this to place constraints on f_{PBH}. We discuss the influence of a deviation from the assumptions used in calculating the constraints and show that this does not qualitatively change our results.

II. GRAVITATIONAL WAVES FROM MERGING BLACK HOLES

Coalescing binary BHs emit GWs with a characteristic spectrum $dE_{\mathrm{GW}}/d\nu$, with a total energy that makes up a significant fraction of the rest mass [31]. For BHs with identical masses and negligible spins, e.g., one expects $E_{\mathrm{GW}}/M_{2\mathrm{BH}} \simeq 5\%$, where $M_{2\mathrm{BH}}$ is the initial mass of the system. For the ten events observed so far by LIGO, this number ranges between 3.3% and 5.4% [32].

In the following we will study the cumulative effect of all mergers throughout the cosmological evolution. The resulting present energy density *per logarithmic frequency interval* is conventionally expressed in units of the critical density, $\rho_c = 3H_0^2/(8\pi G)$, and computed as [33,34]

$$\Omega_{\mathrm{GW}}(\nu) = \frac{1}{\rho_c} \int_0^\infty d\tilde{z} \int dR(\tilde{z}) \frac{\nu}{(1+\tilde{z})H(\tilde{z})} \frac{dE_{\mathrm{GW}}}{d\nu_s}. \quad (1)$$

Here, the merger rate is denoted as $R(z)$, where z is the cosmological redshift, H is the Hubble rate, and the observed frequency ν corresponds to an emission frequency of $\nu_s = \nu(1+z)$. The *total* energy density in gravitational waves at any given redshift $z \equiv 1/a - 1$ is, therefore,

$$\frac{\rho_{\mathrm{GW}}(z)}{(1+z)^4} = \int_z^\infty d\tilde{z} \int d\nu \int dR(\tilde{z}) \frac{dE_{\mathrm{GW}}/d\nu}{(1+\tilde{z})^2 H(\tilde{z})}. \quad (2)$$

Covariant conservation of energy implies that the mass density in PBHs must correspondingly decrease as $a^{-3}d(a^3\rho_{\mathrm{PBH}}) = -a^{-4}d(a^4\rho_{\mathrm{GW}})$ [35], which gives

$$\frac{\rho_{\mathrm{PBH}}(z)}{(1+z)^3} = C - \int_z^\infty d\tilde{z} \int d\nu \int dR(\tilde{z}) \frac{dE_{\mathrm{GW}}/d\nu}{(1+\tilde{z})H(\tilde{z})}. \quad (3)$$

We fix the integration constant C such that $f_{\mathrm{PBH}} \equiv (\rho_{\mathrm{PBH}}/\rho_{\mathrm{DM}})_{z_{\mathrm{CMB}}}$ is the PBH fraction at $z = z_{\mathrm{CMB}} \simeq 1100$. For the spectrum $dE_{\mathrm{GW}}/d\nu$ we use commonly adopted fitting formulas [36–39].

III. MERGER RATES AND CLUSTERING

In the early Universe, PBH binary formation starts once the Newtonian force between two initial PBHs overcomes

the Hubble flow, with a nearby third PBH providing the angular momentum necessary to prevent a head-on collision [9,40,41]. Later, peculiar velocities may be too large for this to happen; instead, binary formation can be triggered by the energy loss in GWs during close encounters of two PBHs [42,43]. For the parameter combinations of interest to us, though, the rate associated with the first formation mechanism by far exceeds that for the second, even for binaries merging only today [27]. Once formed, these binary systems survive until they merge, largely unaffected by the evolution of the surrounding Universe [44].

A crucial input for calculating those merger rates is the initial clustering of PBHs. Phenomenologically, this can be described in terms of an idealized two-point correlation function $\xi_{\mathrm{PBH}}(r)$ that is constant at scales relevant for the formation of PBH binaries [27]:

$$1 + \xi_{\mathrm{PBH}}(r) \approx \delta_{\mathrm{dc}} = \mathrm{const}, \quad (4)$$

where δ_{dc} describes the local density contrast, evaluated at the time when the two BHs decouple from the Hubble expansion. A perfectly homogeneous PBH distribution corresponds to $\delta_{\mathrm{dc}} = 1$, while a highly clustered PBH distribution is described by $\delta_{\mathrm{dc}} \gg 1$. Values of $\delta_{\mathrm{dc}} \gtrsim 10^5$ are particularly interesting, as they are required to circumvent the tight constraints on PBH DM from microlensing and the CMB [16]. Furthermore, constraints arising from the conversion of PBH DM into gravitational radiation are alleviated if PBH mergers occur only at high redshift, which was demonstrated to happen for $\delta_{\mathrm{dc}} \gtrsim 10^4$ assuming only a single merger step [27].

We will see that a highly clustered initial PBH population not only leads to a more efficient formation of binaries but also to a significantly enhanced merger rate, during the whole cosmological evolution until today. These findings crucially extend previous results in the literature (see, e.g., [27,28]), which consider the impact of clustering only on a single merger step.

IV. CASCADING BLACK HOLE MERGER EVENTS

We thus need to improve these scenarios by allowing for subsequent merger steps, i.e., binary mergers of systems of previously merged PBHs. For simplicity, we model the PBHS distribution as an *initially* monochromatic mass distribution peaked at m_0 and assume that the PBH masses in merger step j are given by

$$m_j = 2m_{j-1} - E_{\mathrm{GW}}(m_{j-1}) \sim 1.9^j m_0. \quad (5)$$

The impact of more realistic, extended initial mass functions is discussed in Sec. IX, where we demonstrate that our key results are not affected by this choice. The average PBH number density $n_j = \rho_{\mathrm{PBH},\infty}/(2^j m_0)$ is locally enhanced by a factor of $1 + \xi(r) \approx \delta_{\mathrm{dc},j}$, where $\rho_{\mathrm{PBH},\infty}$

denotes the initial PBH density and we model the decrease of the PBH clustering as $\delta_{\mathrm{dc},j} \simeq 2^{-j}\delta_{\mathrm{dc},0}$. The details of this decrease will in general depend on the exact form of the two-point correlation function; as argued in Sec. IX, the specific choice above leads to rather conservative limits on the fraction of PBH DM.

The merger rate of the jth merger step is given by

$$R_j(t) = \int_0^{\tilde{x}} dx \int_{\tilde{x}}^{\infty} dy \, \frac{\partial^2 n_{3,j}(x,y)}{\partial x \partial y} \delta(t - \tau(x,y,m_j))$$
$$- \max(t_{\mathrm{dc},j}(x), t_{\mathrm{form}})), \qquad (6)$$

where x and y denote the comoving distances from a given PBH to the nearest and next-to-nearest PBH, respectively, and the number density of PBH triples $n_{3,j}(x,y)$ is given by [27]

$$dn_{3,j}(x,y) = \frac{n_j}{2} e^{-\frac{4\pi}{3}y^3 n_j \delta_{\mathrm{dc},j}} (4\pi n_j \delta_{\mathrm{dc},j})^2 x^2 y^2 dx dy. \quad (7)$$

The delta distribution in Eq. (6) ensures that the coalescence time τ [45],

$$\tau(x,y,m_j) = \tilde{\tau}_j (x/\tilde{x}_j)^{37}(y/\tilde{x}_j)^{-21}, \qquad (8)$$

with

$$\tilde{\tau}_j = \frac{3a_{\mathrm{eq}}^4 \tilde{x}_j^4}{170(Gm_j)^3}, \qquad \tilde{x}_j^3 = \frac{3}{4\pi}\frac{2m_j}{a_{\mathrm{eq}}^3 \rho_{\mathrm{eq}}}, \qquad (9)$$

is measured from when the PBHs are both formed (t_{form}) and decoupled from the Hubble flow ($t_{\mathrm{dc},j}$). PBHs form almost immediately after the corresponding density perturbations enter the Hubble horizon, with a mass m_0 equaling the total energy within the horizon at that time, and the decoupling from the Hubble flow occurs when the gravitational attraction overcomes the Hubble expansion:

$$t_{\mathrm{form}} = Gm_0, \qquad t_{\mathrm{dc},j} = \left(\frac{16\pi G}{3}\rho_{\mathrm{eq}}\right)^{-1/2}\left(\frac{x}{\tilde{x}_j}\right)^6. \qquad (10)$$

The subscript "eq" above refers to matter radiation equality. The merger rates R_j in Eq. (6) are connected to the differential one employed in Eqs. (1)–(3) via

$$dR(\tilde{z}) = \sum_j R_j(t(\tilde{z}))\delta(m - m_j)dm. \qquad (11)$$

To recap, we consider a scenario of subsequent equal-mass mergers with a corresponding shift in the mass distribution and local density contrast in each merger step. Let us stress that even though there are characteristic timescales implied by the merger rates, we allow PBHs of given mass m_j to merge at any time between the decoupling for the jth step (as long as $t_{\mathrm{dc},j} > t_{\mathrm{form}}$) and today. For rare very early mergers this may lead to situations where coalescence in our model begins when, in reality, instead of the eventually merging two PBHs,
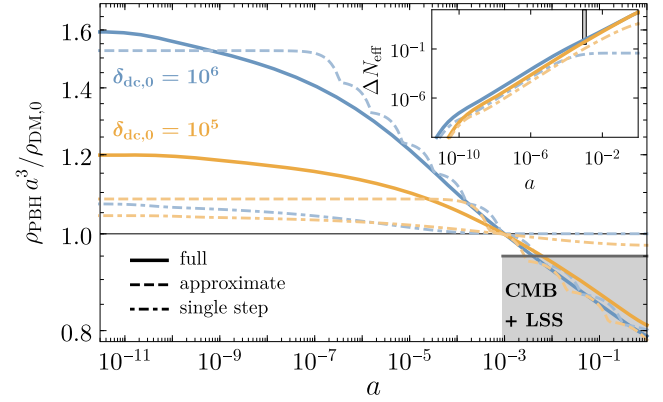

FIG. 1. Conversion of PBH energy density (main panel) into gravitational wave radiation [in terms of a corresponding number ΔN_{eff} of additional neutrinos (inset)] for $m_0 = 1\,M_\odot$, $f_{\mathrm{PBH}} = 1$, and different theoretical treatments. In grey, we indicate regions excluded by cosmology [35].

a preceding set of smaller PBHs is present; in this case, we slightly underestimate the actual amount of emitted GWs. We further introduce an approximate scenario to better visualize the individual merger steps, adopting rates R_j that are zero before $\max(t_{\mathrm{dc},j}, t_{\mathrm{form}})$, constant until the average coalescence time has passed (with average values for x and y), and zero afterwards.

In Fig. 1 we show the decrease of the PBH energy density in our merger scenario (solid lines) as well as the corresponding increase in gravitational wave radiation (inset). Overall, the agreement between the full rates, as computed from Eq. (6), and the simple approximate scenario mentioned above (dashed lines) is fairly good. In particular we note the sizable equidistant spacing of the merger steps, justifying the assumption of a hierarchical merging scenario. The dashed-dotted curves represent the common assumption of a single merger step. For larger values of $\delta_{\mathrm{dc},0}$, this merger step occurs earlier [27], leading to the tempting conclusion that bounds on the GW production can be evaded since the produced radiation is highly redshifted. As we discuss below, this conclusion clearly no longer holds once multiple merger steps are taken into account.

V. COSMOLOGICAL BOUNDS

The conversion of PBH DM into GW radiation modifies the standard cosmological evolution and is constrained by CMB and large scale structure (LSS) observations [35]. These modifications can be roughly split into (i) an upper bound on the effective number of neutrino species at the time of the CMB, $\Delta N_{\mathrm{eff}}(z_{\mathrm{CMB}}) \lesssim 0.3$ [30], indicated by the grey area in the inlet of Fig. 1, and (ii) the amount of DM converted into invisible ("dark") radiation at later times. From Fig. 6 in Ref. [35] one can deduce that not more than $\sim 5\%$ of DM can be converted into dark radiation after the

CMB epoch, irrespective of the precise time dependence of this conversion (and consistent with the 4.2% found for the case of decaying DM [46]). For simplicity, and because other constraints turn out to be stronger, we conservatively adopt this bound of 5% in our analysis (indicated by the grey region in the bottom right of Fig. 1).

VI. THE STOCHASTIC GRAVITATIONAL WAVE BACKGROUND

With the cumulative merger rate described above, it is also straightforward to compute the resulting SGWB as given in Eq. (1). In Fig. 2, we illustrate the predictions for an initial PBH mass of $1\,M_\odot$ and different initial clusterings $\delta_{dc,0} = 10^5$ and $\delta_{dc,0} = 10^6$. The GW spectrum is dominated by late time mergers ($z \lesssim 10$), since earlier GW emission is highly diluted by cosmic expansion. Larger clustering implies that most of these late mergers are associated with heavier BHs, which emit GWs with lower frequencies. For the parameter example of Fig. 2 we find that the mergers occurring at $z = 0$ have typically undergone four (nine) previous mergers for $\delta_{dc,0} = 10^5(10^6)$, resulting in a PBH mass today of around 13 (300) $M_\odot$. Since the frequency of the emitted GWs roughly scales as $\nu \sim 1/M_{2BH}$ (cf. [27,47]), this explains the shift between the two solid lines in Fig. 2. Moreover, the merger cascade described above leads to a mild broadening of the high frequency peak. At low frequencies, the $\Omega_{GW} \sim \nu^{2/3}$ scaling indicates the early inspiral phase of the BH binaries [37].

For comparison, the dashed-dotted curves show the predictions for a single merger step, where the main effect of large clustering is to shift the merging time to high redshift, strongly suppressing the GW spectrum. However, as Fig. 2 demonstrates, later mergers completely change the
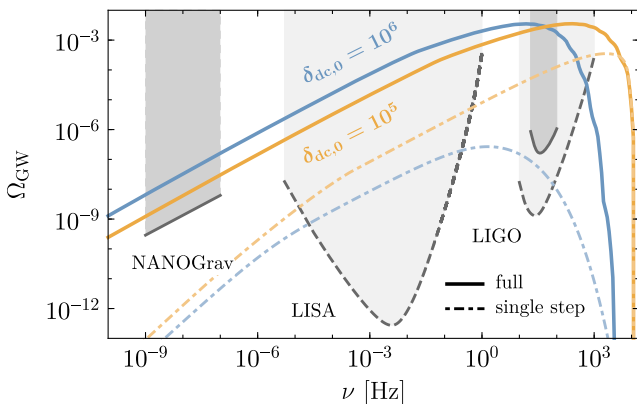

FIG. 2. GW density parameter per logarithmic frequency interval for $m_0 = 1\,M_\odot$, $f_{PBH} = 1$, and different theoretical treatments. In grey, we indicate present (solid lower lines) and projected (dashed lower lines) constraints from NANOGrav [48], LISA [49], and LIGO [50] (present O1 and projected design constraint).

TABLE I. 90% C.L. upper limits on merger rates in the late Universe, taken from Refs. [51–54].

$m/M_\odot$	0.2	1	10	20	40	100	200	300
$R\mathrm{Gpc}^3\,\mathrm{yr}$	10^6	1.9×10^4	330	77	15	2	5	20

picture, leading to a large contribution to the SGWB. The grey contours, finally, indicate the power-law integrated sensitivity curves of LIGO [50] and the pulsar timing array NANOGrav [48], as well as the planned space-based LISA [49] observatory.

VII. OBSERVED MERGER RATE

The LIGO/VIRGO observations strongly constrain the merger rate of PBHs with masses between 0.2 and 300 $M_\odot$ [51–54]. Interpolating linearly between the limiting rates stated in Table I, and comparing this to the calculated $R_j(z = 0)$, allows us to derive an upper bound on f_{PBH}. Starting with an initially monochromatic mass function, we would not expect to reproduce the BH mass distribution observed by LIGO. However, requiring to reproduce the total observed merger rate (12–213 Gpc^{-3} yr^{-1} [15]) with PBH mergers in the sensitivity band of LIGO (7–50 $M_\odot$), we obtain a (very conservative) range in m_0 compatible with the total merger rate observed by LIGO.

VIII. RESULTS

In the left panel of Fig. 3, we summarize the resulting constraints on the allowed fraction of DM in PBHs for large initial clustering, $\delta_{dc,0} = 10^6$, as a function of the initial PBH mass m_0 (the shaded regions are excluded). For reference, we also indicate contour lines with the present, rate-averaged PBH mass m_{avg}. We depict as blue-green and orange curves, respectively, the cosmological constraints [35] indicated as the grey shaded areas in Fig. 1. The blue solid line shows the merger rate constraint; we note that it extends to *average* PBH masses well below the LIGO/VIRGO limit because a small fraction of PBHs will still satisfy $m_{PBH} > 0.2\,M_\odot$ after many merger steps. The remaining lines, finally, correspond to the SGWB constraints from NANOGrav (green) and LIGO (purple) indicated in Fig. 2. The upcoming space-based LISA experiment (red dashed line) may severely tighten these constraints.

In the right panel of Fig. 3, we show our combined results on f_{PBH}, illustrating that larger values of the clustering parameter $\delta_{dc,0}$ in fact lead to tighter constraints. For comparison, the dashed-dotted lines indicate the much weaker constraints obtained when taking into account only a single merger step. The arrows indicate the range for m_0, where for a suitable f_{PBH} the total present merger rate is consistent with all observed LIGO events being caused by PBH mergers.
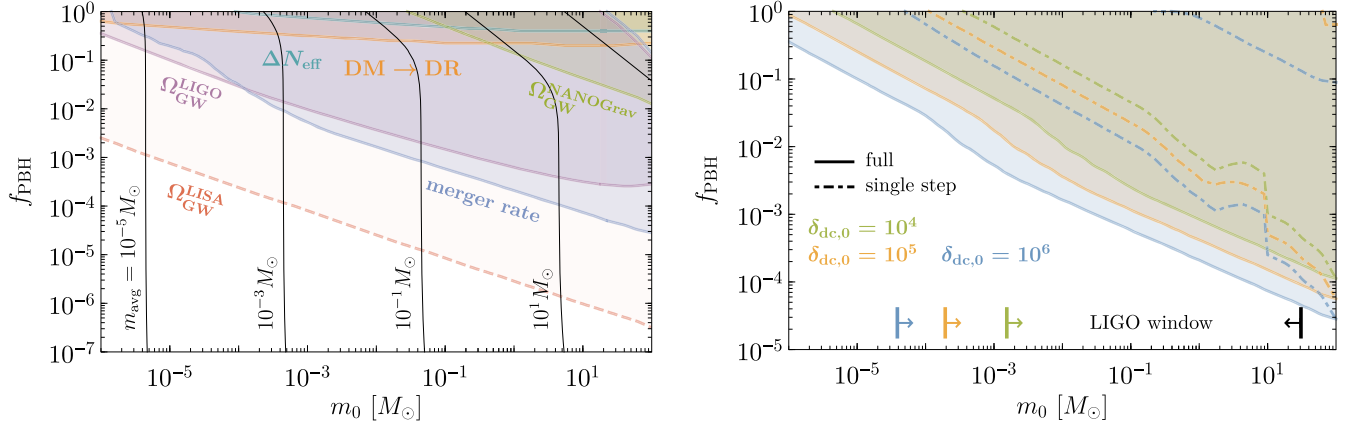
FIG. 3. Left: Constraints on the allowed fraction f_{PBH} of PBH DM as a function of the initial PBH mass m_0 for large clustering ($\delta_{dc,0} = 10^6$) in the merger cascade scenario. The thinner black lines indicate contours of the rate-averaged PBH mass $m_{avg} = (\sum_j R_j m_j)/\sum_j R_j$ at $z = 0$. Right: Combined constraints on f_{PBH} for different clustering parameters $\delta_{dc,0}$.

IX. DISCUSSION

We made a number of simplifying assumptions when modeling the PBH merger history, which can impact the details of the limits summarized in Fig. 3. As we argue below, however, our main result that a large clustering leads to a *tightening* of existing limits is robust. This implies, in particular, that the BHs observed by LIGO cannot be part of a PBH population comprising all of the DM.

A. Extended mass distributions

In the above calculation, we focused for simplicity on an initially monochromatic PBH mass distribution. Realistic models of PBH formation, however, predict extended mass functions. For example, if the scalar perturbations which collapse into PBHs are formed during single-field inflation, then the characteristic timescale governing the width of any peaked feature in the scalar power spectrum is the Hubble time. Consequently, the resulting PBH mass distribution is expected to be rather broad, since the range of enhanced length scales is exponentially sensitive to this timescale [55] (though notable exceptions exist [56–59]). More generally, even if the spectrum of enhanced scalar perturbations is essentially monochromatic, the process of collapsing the initial perturbations into PBHs obeys a critical scaling relation, implying a finite width for the resulting PBH mass spectrum [5]. Here we discuss how the results in the main text are affected by relaxing the assumptions of an initially monochromatic PBH mass distribution.

To model an extended PBH mass function, we consider the log-normal mass distribution

$$\psi_{log}(m) = \frac{f_{PBH,\infty}}{\sqrt{2\pi}\sigma m} \exp\left(\frac{\log^2(m/m_0)}{2\sigma^2}\right), \qquad (12)$$

where σ encodes the width of the distribution centered around the reference scale m_0. This distribution is

normalized so that $f_{PBH,\infty} = \int_0^\infty dm\, \psi(m)$. Note that for computational simplicity, we fix the PBH fraction of DM at $z \to \infty$ in this section as indicated by the subscript ∞. In our scenario of multiple mergers, the strongest constraints on the PBH abundance arise from the bounds on the SGWB and from the observed merger rate in LIGO; see Fig. 3. Consequently we will focus on the impact of the distribution (12) on these two quantities, noting that in particular significant changes in the (hierarchy of) the merger rates at the individual steps could potentially entail significant changes in our computations.

Figure 4 shows the time evolution of the merger rate (integrated over all masses) for different mass distributions for a *single* merger step, obtained by reinstating an extended mass function in Eq. (6). Here, the coalescence time depends on the masses of the PBHs in the binary ($m^{(1)}$ and $m^{(2)}$) and the third PBH ($m^{(3)}$) providing angular momentum, and the number density of PBH triples is now given by
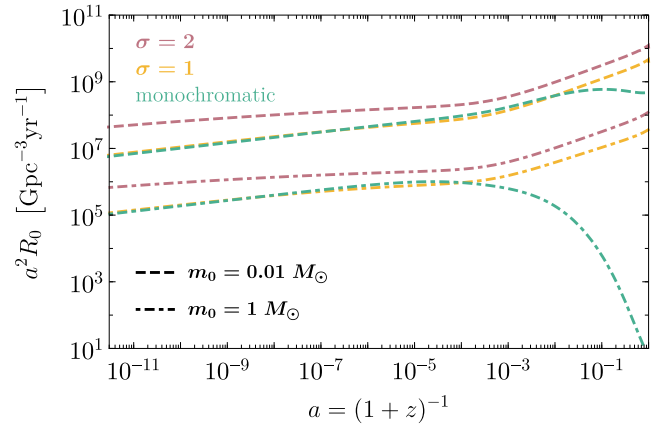

FIG. 4. Evolution of mass-integrated merger rate for log-normal mass distributions with $\sigma = 1$ and 2 and monochromatic mass distributions considering only one step with $f_{PBH} = 1$, $\delta_{dc,0} = 10^6$. Note the additional factor of a^2 on the y-axis.

$$dn_{3,0}^{\log/\mathrm{mono}}(x,y) = \frac{\rho_{\mathrm{PBH},\infty}}{2}e^{-N(y)}(4\pi\rho_{\mathrm{PBH},\infty}\delta_{\mathrm{dc},0})^2$$

$$\times\, x^2 y^2 dx dy \prod_{i=1}^{3}\frac{\psi_{\log/\mathrm{mono}}}{m^{(i)}}dm^{(i)}, \quad (13)$$

where

$$\rho_{\mathrm{PBH},\infty} = \lim_{z\to\infty}(1+z)^{-3}\rho_{\mathrm{PBH}}(z), \quad (14)$$

$$N(y) = \int_0^y d\tilde{y}\int_0^m d\tilde{m}$$

$$4\pi\tilde{y}^2\delta_{\mathrm{dc},0}\rho_{\mathrm{PBH},\infty}\frac{\psi_{\log/\mathrm{mono}}(\tilde{m})}{\tilde{m}}, \quad (15)$$

$$\psi_{\mathrm{mono}}(m) = f_{\mathrm{PBH},\infty}\delta(m - m_0). \quad (16)$$

For more details see [27]. We note that the time evolution of this merger rate does not change significantly when going from a monochromatic to a log-normal mass distribution. This situation only changes at very late times, when the merger rate of this single merger step has however anyway dropped to a small value (note the additional factor of a^2 in Fig. 4). For the density contrast employed in Fig. 4, $\delta_{\mathrm{dc},0} = 10^6$, subsequent steps start to dominate the total merger rate for $a \gtrsim 5\times 10^{-5}$ and $a \gtrsim 10^{-6}$ for $m_0 = 0.01\,M_\odot$ and $m_0 = 1\,M_\odot$, respectively. In conclusion, neither the hierarchy among the merger times of the individual merger steps nor the total amount of mergers is significantly altered when assuming a rather narrow log-normal mass distribution. For broader distributions the rate is even enhanced.

The SGWB for the log-normal distribution (12) was studied in [27] for a single merger step, finding (for $\sigma = 1$) a similar GW spectrum as in the monochromatic case. Since the GW radiation from early PBH mergers experiences a significant redshift, the SGWB in the multiple merger scenario is dominated by the very last merger. Consequently, since we found above that the overall merger history is not significantly altered in the case of a log-normal mass distribution, we conclude that also the resulting SGWB is only moderately altered.

In summary, the strongest constraints depicted in Fig. 3 do not appear to be very sensitive to the assumption of a monochromatic initial PBH mass function. Depending on the mass function in question, they may vary by a factor of a few or even an order of magnitude, but the option of obtaining a significant PBH dark matter fraction in the LIGO window of ~10 $M_\odot$ remains firmly excluded. For a given peaked mass distribution one may conservatively estimate the constraints on highly clustered PBH dark matter by considering a narrow window around the central mass value, and applying the analysis of the main text to this window only.

B. Decrease of local density contrast

An important parameter in the modeling of the multiple merger scenario is the decrease in the local density contrast δ_{dc}, which depends on the details of the two-point correlation function. In a large PBH "cloud" of constant density, the (number) density contrast stays approximately constant through many merger steps. On the contrary, for PBH "clouds" in which the typical distance from one PBH binary to the next is enhanced compared to the initial size of the binary, the density contrast drops faster. In the above calculation, we considered $\delta_{\mathrm{dc,j}} = 0.5^j\delta_{\mathrm{dc},0}$, which we consider a conservative approach for highly clustered PBH distributions.

Here we also discuss the case of a locally approximately homogeneous density contrast. To model this, we consider $\delta_{\mathrm{dc,j}} = 0.9^j\delta_{\mathrm{dc},0}$. The resulting constraints, depicted in Fig. 5 for $\delta_{\mathrm{dc},0} = 10^3$, are clearly significantly tighter than those presented in Fig. 3. Note that in this case the bounds can be extrapolated down to very low masses. Taken at face value, this even allows us to constrain masses as low as $m_0 = 10^{-16}\,M_\odot$, but this extrapolation implicitly assumes very large overdensities of $\mathcal{O}(10^{15})$ PBHs, which seems hardly realistic. We also note that such a slow decrease in the density contrast weakens the hierarchy between the merger times of the individual merger steps, making our analysis less robust.

We conclude this section by noting that for this slower decrease in the density contrast corresponding to rather homogeneous PBH "clouds," the formation of N-body systems may lead to a more complicated merger history not covered by the treatment in this work [60].

C. Gravitational wave recoil

Due to asymmetries in the emitted gravitational radiation, the remnant of merging binary BHs can gain recoil velocities of $\mathcal{O}(100\text{–}1000\text{ km/s})$ [61–63]. These velocities are zero in the equal-mass zero-spin case, but differ from
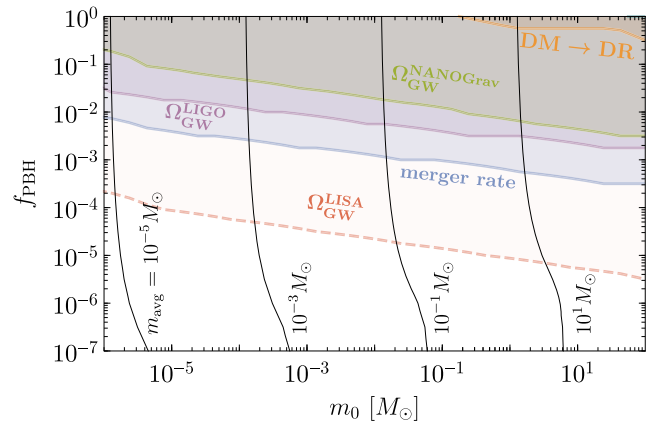

FIG. 5. Constraints for smaller initial clustering, $\delta_{\mathrm{dc},0} = 10^3$ and $\delta_{\mathrm{dc,j}} = 0.9^j\delta_{\mathrm{dc},0}$. See Fig. 3 for details.

zero if either of these conditions is not met. Specifically, a maximal velocity of ~175 km/s can be obtained in the zero-spin case for a BH mass ratio of 0.36. For equal masses and nonzero spins with special alignment the maximum recoil velocity can be as large as ~5000 km/s [63]. As special spin alignment is unlikely in the context of this work, we expect recoil velocities of $\mathcal{O}(100 \text{ km/s})$. In our treatment of multiple merger steps we have implicitly assumed that recoils do not affect the evolution of the PBHs. Here we show that this approximation is justified, by comparing these recoil velocities to the relevant escape velocities.

The escape velocity from a PBH cluster will depend on its global structure and hence on the two-point correlation function. As we take the local density contrast to decrease as $\delta_{\text{dc},j} \simeq 2^{-j}\delta_{\text{dc},0}$, we expect initial clusters to contain $\sim\delta_{\text{dc},0}$ PBHs with comoving radius $x_{\text{clus}} = (3/4\pi n_0)^{1/3}$, such that $4\pi x_{\text{clus}}^3 n_0 \delta_{\text{dc},0}/3 = \delta_{\text{dc},0}$. These clusters decouple from the Hubble flow during radiation domination when the local energy density in PBHs $\rho_{\text{PBH}}\delta_{\text{dc},0}$ is equal to the background density. This gives a decoupling scale factor and an escape velocity from the cluster of

$$a_{\text{dc,clus}} = a_{\text{eq}}^4 \frac{\rho_{\text{eq}}}{2m_0 n_0 \delta_{\text{dc},0}}, \qquad (17)$$

$$v_{\text{esc,clus}} \simeq \sqrt{\frac{2G\delta_{\text{dc},0}m_0}{x_{\text{clus}}a_{\text{dc,clus}}}}$$
$$= 3600 \frac{\text{km}}{\text{s}} f_{\text{PBH}}^{2/3} \left(\frac{m_0}{M_\odot}\right)^{1/3} \frac{\delta_{\text{dc},0}}{10^4}. \qquad (18)$$

This implies that for most regions of parameter space recoils should not affect our results.

This conclusion may seemingly be challenged for small initial masses and small values of f_{PBH}. In this case, however, our constraints are driven by rare events of many merger steps, implying that initially the PBHs were exceptionally close. Specifically note that any mergers we take into account in our limits must have a coalescence time τ smaller than the age of the Universe t_0, i.e.,

$$\tau = \tilde{\tau}_j(x/\tilde{x}_j)^{37}(y/\tilde{x}_j)^{-21} \leq t_0. \qquad (19)$$

Conservatively estimating $y \simeq 2^{1/3}x$ [smaller values give larger escape velocities and larger values are exponentially suppressed by the exponential term in Eq. (7)], the escape velocity from a binary BH in merger step j can be written as

$$v_{\text{esc,bin}} = \sqrt{\frac{2Gm_j}{xa_{\text{dc},j}}} \gtrsim 190 \frac{\text{km}}{\text{s}} \left(\frac{m_j}{M_\odot}\right)^{1/8}, \qquad (20)$$

where $a_{\text{dc},j}$ is the scale factor at which the binary system decouples from the Hubble flow. We see that PBHs with $m_j \gtrsim 0.1\,M_\odot$, which are relevant for the merger rate and the stochastic GW background from LIGO, typically do not pick up a sufficient recoil in their previous merger to escape the gravitational attraction of even their nearest neighbor. Note however that even subcritical recoils as well as gravitational scattering will generally lead to dynamical heating. A detailed analysis of this effect is beyond the scope of this work.

In summary, due to the early formation time, the relevant PBH escape velocities are very large in the highly clustered scenarios we have studied here, allowing us to neglect the effect of GW recoils in our analysis.

X. CONCLUSIONS

If PBHs are not homogeneously distributed in the Universe but highly clustered, existing bounds on their abundance must be reinterpreted. Here we have demonstrated that the resulting limits are not weakened, as claimed previously, but instead strengthened because subsequent merger steps would dominate the SGWB. Taking into account constraints from cosmology and direct GW searches, we find that for $\delta_{\text{dc},0} > 10^4$ the case of pure PBH DM is firmly excluded in the entire range of initial PBH masses between $10^{-5}\,M_\odot$ and $100\,M_\odot$. For slightly less conservative assumptions about the decrease of δ_{dc} in subsequent merger steps, this even holds for much smaller initial density contrasts. We note that outside this mass range bounds are also very strong [10], which essentially left this interval as one out of only two realistic options for explaining all DM in terms of PBHs (the second one arises for much lighter PBHs of $10^{-16} \lesssim m_{\text{PBH}}/M_\odot \lesssim 10^{-11}$ [64]).

Note added.—After this work was finished, [60] appeared as a preprint and reopened the question of the stability of PBH binary systems with respect to perturbations by nearby PBHs, which could in particular influence the merger rates entering our results. A detailed analysis of this effect in the context of multiple mergers, which most likely requires N-body simulations, is still to be performed.

---

[1] Y. B. Zel'dovich and I. D. Novikov, Sov. Astron. **10**, 602 (1967).

[2] S. Hawking, Mon. Not. R. Astron. Soc. **152**, 75 (1971).

[3] B. J. Carr and S. W. Hawking, Mon. Not. R. Astron. Soc. **168**, 399 (1974).

[4] G. F. Chapline, Nature (London) **253**, 251 (1975).

[5] B. Carr, F. Kuhnel, and M. Sandstad, Phys. Rev. D **94**, 083504 (2016).

[6] M. Sasaki, T. Suyama, T. Tanaka, and S. Yokoyama, Classical Quantum Gravity **35**, 063001 (2018).

[7] S. Bird, I. Cholis, J. B. Muñoz, Y. Ali-Haïmoud, M. Kamionkowski, E. D. Kovetz, A. Raccanelli, and A. G. Riess, Phys. Rev. Lett. **116**, 201301 (2016).

[8] S. Clesse and J. García-Bellido, Phys. Dark Universe **15**, 142 (2017).

[9] M. Sasaki, T. Suyama, T. Tanaka, and S. Yokoyama, Phys. Rev. Lett. **117**, 061101 (2016); **121**, 059901(E) (2018).

[10] B. Carr, M. Raidal, T. Tenkanen, V. Vaskonen, and H. Veermäe, Phys. Rev. D **96**, 023514 (2017).

[11] S. Wang, Y.-F. Wang, Q.-G. Huang, and T. G. F. Li, Phys. Rev. Lett. **120**, 191102 (2018).

[12] B. P. Abbott et al. (Virgo and LIGO Scientific Collaborations), Phys. Rev. Lett. **116**, 061102 (2016).

[13] B. P. Abbott et al. (Virgo and LIGO Scientific Collaborations), Phys. Rev. Lett. **116**, 241103 (2016).

[14] B. P. Abbott et al. (Virgo and LIGO Scientific Collaborations), Phys. Rev. X **6**, 041015 (2016).

[15] B. P. Abbott et al. (VIRGO and LIGO Scientific Collaborations), Phys. Rev. Lett. **118**, 221101 (2017).

[16] J. García-Bellido and S. Clesse, Phys. Dark Universe **19**, 144 (2018).

[17] M. Zumalacarregui and U. Seljak, Phys. Rev. Lett. **121**, 141101 (2018).

[18] J. Garcia-Bellido, S. Clesse, and P. Fleury, Phys. Dark Universe **20**, 95 (2018).

[19] J. R. Chisholm, Phys. Rev. D **73**, 083504 (2006).

[20] J. R. Chisholm, Phys. Rev. D **84**, 124031 (2011).

[21] V. Dokuchaev, Y. Eroshenko, and S. Rubin, Gravitation Cosmol. **11**, 99 (2005).

[22] V. I. Dokuchaev, Yu. N. Eroshenko, and S. G. Rubin, arXiv:0709.0070.

[23] Y. Ali-Haïmoud, Phys. Rev. Lett. **121**, 081304 (2018).

[24] V. Desjacques and A. Riotto, Phys. Rev. D **98**, 123533 (2018).

[25] S. Young and C. T. Byrnes, Phys. Rev. D **91**, 083521 (2015).

[26] K. M. Belotsky, V. I. Dokuchaev, Y. N. Eroshenko, E. A. Esipova, M. Yu. Khlopov, L. A. Khromykh, A. A. Kirillov, V. V. Nikulin, S. G. Rubin, and I. V. Svadkovsky, arXiv:1807.06590.

[27] M. Raidal, V. Vaskonen, and H. Veermäe, J. Cosmol. Astropart. Phys. 09 (2017) 037.

[28] G. Ballesteros, P. D. Serpico, and M. Taoso, J. Cosmol. Astropart. Phys. 10 (2018) 043.

[29] B. Carr and J. Silk, Mon. Not. R. Astron. Soc. **478**, 3756 (2018).

[30] N. Aghanim et al. (Planck Collaboration), arXiv:1807.06209.

[31] M. Maggiore, *Gravitational Waves. Vol. 2: Astrophysics and Cosmology* (Oxford University Press, Oxford, 2018).

[32] B. P. Abbott et al. (LIGO Scientific and Virgo Collaborations), arXiv:1811.12907.

[33] E. S. Phinney, arXiv:astro-ph/0108028.

[34] B. P. Abbott et al. (Virgo and LIGO Scientific Collaborations), Phys. Rev. Lett. **116**, 131102 (2016).

[35] T. Bringmann, F. Kahlhoefer, K. Schmidt-Hoberg, and P. Walia, Phys. Rev. D **98**, 023543 (2018).

[36] C. Cutler, E. Poisson, G. J. Sussman, and L. S. Finn, Phys. Rev. D **47**, 1511 (1993).

[37] X.-J. Zhu, E. Howell, T. Regimbau, D. Blair, and Z.-H. Zhu, Astrophys. J. **739**, 86 (2011).

[38] D. F. Chernoff and L. S. Finn, Astrophys. J. **411**, L5 (1993).

[39] P. Ajith et al., Phys. Rev. D **77**, 104017 (2008); **79**, 129901(E) (2009).

[40] T. Nakamura, M. Sasaki, T. Tanaka, and K. S. Thorne, Astrophys. J. **487**, L139 (1997).

[41] K. Ioka, T. Chiba, T. Tanaka, and T. Nakamura, Phys. Rev. D **58**, 063003 (1998).

[42] G. D. Quinlan and S. L. Shapiro, Astrophys. J. **343**, 725 (1989).

[43] H. Mouri and Y. Taniguchi, Astrophys. J. **566**, L17 (2002).

[44] Y. Ali-Haïmoud, E. D. Kovetz, and M. Kamionkowski, Phys. Rev. D **96**, 123523 (2017).

[45] P. C. Peters, Phys. Rev. **136**, B1224 (1964).

[46] V. Poulin, P. D. Serpico, and J. Lesgourgues, J. Cosmol. Astropart. Phys. 08 (2016) 036.

[47] M. Maggiore, *Gravitational Waves. Vol. 1: Theory and Experiments*, Oxford Master Series in Physics (Oxford University Press, Oxford, 2007).

[48] Z. Arzoumanian et al. (NANOGRAV Collaboration), Astrophys. J. **859**, 47 (2018).

[49] H. Audley et al. (LISA Collaboration), arXiv:1702.00786.

[50] B. P. Abbott et al. (Virgo and LIGO Scientific Collaborations), Phys. Rev. Lett. **118**, 121101 (2017); **119**, 029901(E) (2017).

[51] B. P. Abbott *et al.* (Virgo and LIGO Scientific Collaborations), Astrophys. J. **833**, L1 (2016).

[52] B. P. Abbott *et al.* (Virgo and LIGO Scientific Collaborations), Astrophys. J. Suppl. Ser. **227**, 14 (2016).

[53] B. P. Abbott *et al.* (Virgo and LIGO Scientific Collaborations), Phys. Rev. D **96**, 022001 (2017).

[54] B. P. Abbott *et al.* (Virgo and LIGO Scientific Collaborations), Phys. Rev. Lett. **121**, 231103 (2018).

[55] B. J. Carr, K. Kohri, Y. Sendouda, and J. Yokoyama, Phys. Rev. D **81**, 104019 (2010).

[56] A. A. Starobinsky, Pis'ma Zh. Eksp. Teor. Fiz. **55**, 477 (1992) [JETP Lett. **55**, 489 (1992)].

[57] D. Blais, T. Bringmann, C. Kiefer, and D. Polarski, Phys. Rev. D **67**, 024024 (2003).

[58] D. Blais, C. Kiefer, and D. Polarski, Phys. Lett. B **535**, 11 (2002).

[59] N. Orlofsky, A. Pierce, and J. D. Wells, Phys. Rev. D **95**, 063518 (2017).

[60] M. Raidal, C. Spethmann, V. Vaskonen, and H. Veermäe, J. Cosmol. Astropart. Phys. 02 (2019) 018.

[61] M. Koppitz, D. Pollney, C. Reisswig, L. Rezzolla, J. Thornburg, P. Diener, and E. Schnetter, Phys. Rev. Lett. **99**, 041102 (2007).

[62] L. Rezzolla, E. N. Dorband, C. Reisswig, P. Diener, D. Pollney, E. Schnetter, and B. Szilagyi, Astrophys. J. **679**, 1422 (2008).

[63] C. O. Lousto and Y. Zlochower, Phys. Rev. Lett. **107**, 231102 (2011).

[64] H. Niikura *et al.*, arXiv:1701.02151.